Magnetic-Field Induced Second Harmonic Generation in CuB_2O_4

R. V. Pisarev,[1] I. Sänger,[2] G. A. Petrakovskii,[3] and M. Fiebig[4,*]

[1]*Ioffe Physical Technical Institute of the Russian Academy of Sciences, 194021 St. Petersburg, Russia*
[2]*Institut für Physik, Universität Dortmund, 44221 Dortmund, Germany*
[3]*Siberian Branch of the Russian Academy of Sciences, Institute of Physics, 660036 Krasnoyarsk, Russia*
[4]*Max-Born-Institut, Max-Born-Straße 2A, 12489 Berlin, Germany*

(Received 26 January 2004; published 15 July 2004)

Three types of optical magnetic-field induced second harmonic (MFISH) generation are observed in CuB_2O_4. Unusually sharp and intense electronic transitions in MFISH and linear absorption spectra provide selective access to the two nonequivalent Cu^{2+} sublattices. The magnetic phase diagram for both sublattices is determined by MFISH. Magnetic structure is dominated by antiferromagnetic order at the 4*b* site. Sublattice interactions transfer it to the 8*d* site where it coexists with a discoupled paramagnetic component.

DOI: 10.1103/PhysRevLett.93.037204 PACS numbers: 75.25.+z, 42.65.Ky, 71.70.Ch, 75.30.Kz

Nonlinear optics has been a thriving field of research since the 1960s with second harmonic generation (SHG) as the simplest nonlinear optical process playing a particular role [1,2]. With its larger number of degrees of freedom SHG reveals new and complementary information in comparison to linear optics [3–5]. The leading-order contribution to SHG, in which interaction of light and matter is described as electric-dipole transition, is allowed only in crystals where space inversion symmetry is broken by the distribution of charges or spins [1,3,6]. However, a simple way to induce SHG in centrosymmetric media is an electric field which due to its polar nature breaks inversion symmetry [7]. Such electric-field induced second harmonic (EFISH) was used to study the space-charge region of semiconductor heterostructures, build quasi-phase-matching devices, etc. [8]. In contrast, the axial nature of a magnetic field breaks time-inversion symmetry and should lead to new magnetic-field induced second harmonic (MFISH) contributions allowing one to probe the *spin* (in contrast to the *charge*) of the electron. With the contemporary interest in spintronics devices, complementary use of MFISH and EFISH as a sensor to spintronics properties is self-evident.

In this Letter we report three types of "giant" MFISH effects in the antiferromagnetic two-sublattice compound CuB_2O_4. MFISH intensities allowing naked-eye observation were employed for a detailed comparative analysis of linear and SHG spectra which revealed sublattice selective as well as resonance enhanced contributions. Using MFISH as a probe for the magnetic structure we distinguish between magnetic sublattices, identify their interaction and respective order, and construct the magnetic phase diagram.

Three types of MFISH can be distinguished. (A) Disordered materials or sublattices where the applied magnetic field reduces symmetry in a perturbative way, thus inducing new contributions to SHG. The only known example is a weak surface induced MFISH signal at fixed frequency from Si [9]. (B) Magnetically ordered materials, where the magnetic field induces phase transitions, which lead to new SHG components. Only antiferromagnetic SHG in the spin-flop phase of Cr_2O_3 [10] and the system of hexagonal manganites [11] can serve as examples. (C) Magnetically ordered materials, where the magnetic field increases an existing SHG signal by creating a single-domain state with maximum magnetization. New SHG contributions are not induced. Processes of this type are reviewed in Ref. [12]. They can be counted as MFISH contributions only in a broader sense since the intrinsic magnetic order, not the applied field, is the original source of SHG.

CuB_2O_4 belongs to the class of noncentrosymmetric magnetically ordered materials for which unusual coexistence of "weak" Dzyaloshinskii-Moriya–type ferromagnetism and inhomogeneous (incommensurate) magnetic ordering attracts a lot of attention [13,14]. Unfortunately analysis of magnetic structure in these materials is difficult because of their complexity. Simplified models for the interpretation of diffraction data lead to the proposition of contradictory magnetic structures [14–16]. Therefore, CuB_2O_4 is an ideal candidate material for demonstrating the potential and effectiveness of MFISH. It will be seen that all three MFISH mechanisms are observed with unprecedented clarity and intensity, thus allowing us to determine the magnetic structure.

CuB_2O_4 crystallizes in the tetragonal space group $I\bar{4}2d$ [17]. Cu^{2+} ions at 4*b* sites are surrounded by four oxygen atoms in planar quadratic coordination so that local symmetry is $\bar{4}$. Cu^{2+} ions at 8*d* sites occupy distorted octahedral positions with an exceptionally large separation of 3.069 Å from the two apical O^{2-} ions [17]. Local symmetry is 2. In the ligand field degeneracy of the Cu^{2+} ($3d^9$) eigenstates is lifted. Assuming that (i) energy scales with the degree of overlap between the wave function of the Cu^{2+} and O^{2-} ions, and (ii) influence of the remote apical O^{2-} ions is small the energy levels in Fig. 1 are derived on the basis of Ref. [18]. Note that the original

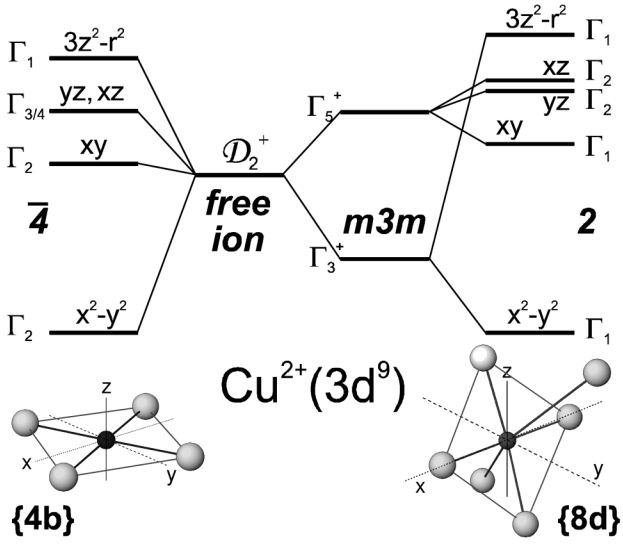

FIG. 1. Electronic states, local symmetry, and coordination of $Cu^{2+}(3d^9)$ ions at 4*b* and 8*d* sites in CuB_2O_4. Wave functions are given in terms of the *local* coordinate system whose axes are defined by the connections between the central Cu^{2+} ion and the square or undistorted octahedron of O^{2-} ligands at the respective sites. Local symmetry is given in bold italics. The sequence of levels is discussed in the text. Coordination is shown for the Cu^{2+} ion (black spheres) with the nearest O^{2-} ligands (gray spheres). Axes are those of the *global* coordinate system.

Cu^{2+} *d*-wave functions are mixed with O^{2-} *p*-wave functions because of broken centrosymmetry. Magnetic properties of CuB_2O_4 originate from the Cu^{2+} spin 1/2 and interaction of 4*b* and 8*d* sublattices. Above $T_N = 21$ K it is paramagnetic. At $10 < T < 21$ K the 4*b* site exhibits commensurate easy-plane antiferromagnetism with weak Dzyaloshinskii-Moriya–type ferromagnetic components [14–16] while the 8*d* site remains disordered according to contemporary belief [14,16,19,20]. Below $T^* = 10$ K incommensurate antiferromagnetism with possible 8*d*-site ordering was found. Another phase transition at $\lesssim 2$ K was reported [21].

CuB_2O_4 bulk single crystals were grown [22], cut, and polished into (110), (010), and (001) platelets with a thickness of 60–100 μm. Absorption was measured in the 1.3–2.5 eV range using a Cary 2300 spectrophotometer and a 0.85 m SPEX monochromator. SHG was investigated in transmission in the 1.2–3.0 eV range using the setup described in Ref. [23].

SHG in the presence of a static magnetic field $\vec{H}^0$ is described by

$$P_i(2\omega) = \epsilon_0 i \chi_{ijkl} E_j(\omega) E_k(\omega) H_l^0, \qquad (1)$$

with $\hat{\chi}$ as MFISH susceptibility which is time invariant ($\hat{T}\hat{\chi} = +\hat{\chi}$ with $\hat{T}$ as time reversal) in the case of A-type MFISH or time noninvariant ($\hat{T}\hat{\chi} = -\hat{\chi}$) in the case of B-type MFISH [24]. $\vec{E}(\omega)$ and $\vec{P}(2\omega)$ represent the electric field of the incident fundamental light and the SH polarization induced in the crystal. Note that a field independent contribution $P_i(2\omega) = \epsilon_0 \chi'_{ijk} E_j(\omega) E_k(\omega)$ is also allowed. However, in general its selection rules are different so that it is suppressed by a suitable choice of polarizations for $\vec{E}(\omega)$ and $\vec{P}(2\omega)$ [see inset in Fig. 2(c)].

Figures 2 and 3 show polarization dependent SH and absorption spectra of CuB_2O_4. The inset in Fig. 2(b) shows an increase of SH intensity in the magnetic field from ≤ 1 at $H = 0$ (1 defining the detection limit) by 3 orders of magnitude. At $\mu_0 H_x = 7$ T this, according to Fig. 4(d), A-type MFISH signal is of the order of magnitude as SHG in crystalline quartz, thus exceeding the only reported effect [9] by many orders of magnitude. The MFISH spectrum displays sets of narrow zero-phonon lines (< 1 meV) corresponding to *d*-*d* transitions of the $Cu^{2+}(3d^9)$ ions. They are accompanied by phonon-assisted transitions forming a broadband (> 100 meV) background. The absorption spectra in Fig. 3 are remarkable: In most wide-gap transition-metal oxides with *d*-*d* transitions below the band gap absorption bands are broad and featureless [25–27]. However, in CuB_2O_4 they reproduce the same coexistence of narrow and broad transitions as in the MFISH spectra with up to 70 well-resolved phonon sidebands.

Comparison of MFISH spectra from χ_{xxxx}, χ_{zxxx}, and χ_{zzzx} reveals three sets of zero-phonon transitions. We observe (i) lines at 1.410, 1.675, and 1.910 eV; (ii) lines at 1.575, 1.875, and 2.120 eV; (iii) a line at 2.820 eV. Set (i)

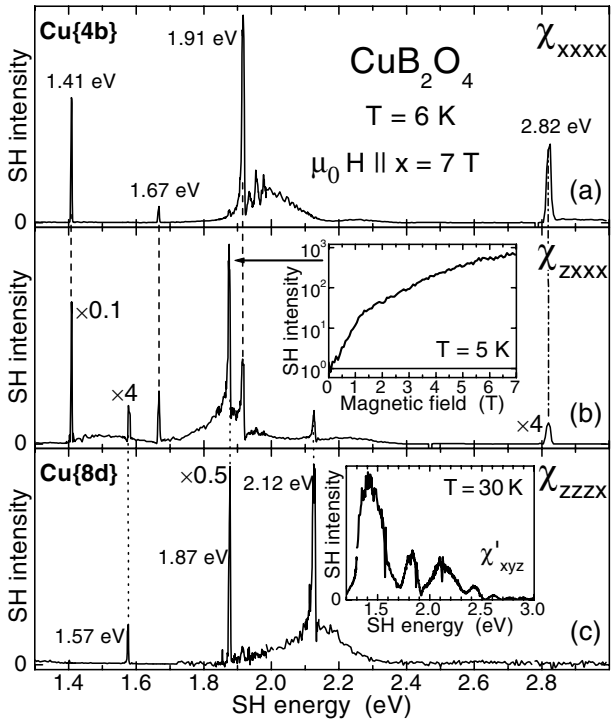

FIG. 2. MFISH spectra of (010) oriented CuB_2O_4 in a static magnetic field applied along the *x* axis. Insets show (b) the magnetic-field dependence of SHG, and (c) the spectral dependence of crystallographic SHG for a (110) oriented sample. Susceptibilities χ_{ijkl} refer to Eq. (1).

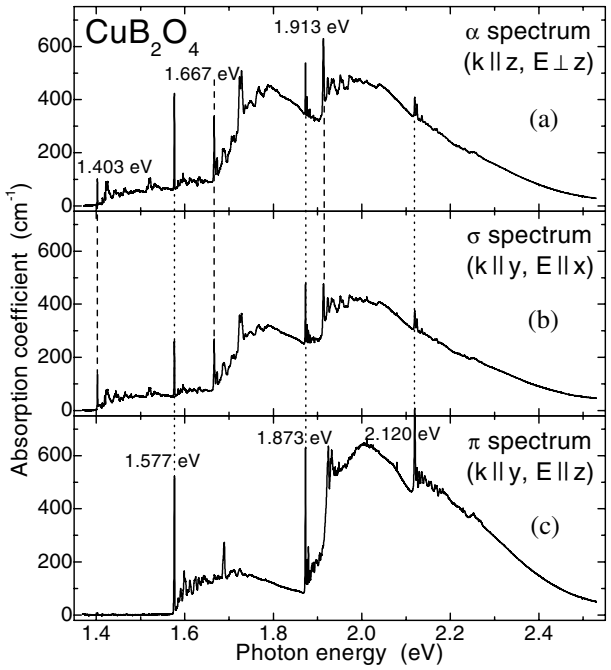

FIG. 3. Linear absorption spectra of (a) (100) oriented and (b),(c) (010) oriented CuB_2O_4 at $H = 0$. k and E denote wave vector and polarization of the incoming light wave at frequency ω.

is associated with transitions of the $Cu^{2+}\{4b\}$ ion. They are reproduced by the χ_{xxxx} and χ_{zxxx} components and by α and σ polarized light in absorption. However, they are absent in the π spectrum because the $Cu^{2+}\{4b\}$ ion and its four O^{2-} ligands form a planar structure in the xy plane which does not couple to z polarized incident light. Set (ii) is associated with transitions of the $Cu^{2+}\{8d\}$ ion. They are reproduced by the χ_{zzzx} and χ_{zxxx} components, and because the $Cu^{2+}\{8d\}$ ion and its six O^{2-} ligands

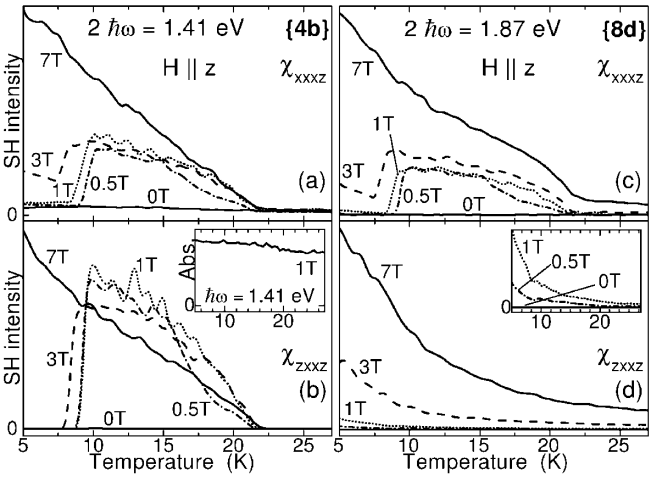

FIG. 4. Temperature dependence of MFISH intensity at (a),(b) 4b and (c),(d) 8d sites in static magnetic fields applied along the z axis of (010) oriented CuB_2O_4. Inset of (b): temperature dependence of linear absorption (Abs.) for $k \parallel y$, $E \parallel x$.

form a tilted three-dimensional unit, light with any polarization is absorbed. Set (iii) contains a sole line at twice the photon energy of the 1.410 eV line from set (i). It originates in a two-photon transition which is enhanced by a resonant single-photon transition to the state at 1.410 eV [23] and does not indicate an electronic state. Note that the spectra in Figs. 2 and 3 are in full agreement with Fig. 1. For both Cu^{2+} sites three transitions from the $x^2 - y^2$ ground state to the xy, yz/xz, and $3z^2 - r^2$ states are observed. Transition energies at 4b and 8d sites are similar because of the small influence of the remote apical O^{2-} ions. Splitting of the yz and xz states at the 8d site is not resolved because it is determined by the variation of Cu^{2+}-O^{2-} in-plane distances which is only 2.6% [17].

A critical limitation of linear optics is revealed by the inset in Fig. 4(b). While absorption displays the lines in Fig. 2 as *electronic* transitions, thus corroborating their site selectivity, it is nonetheless insensitive to *magnetic* ordering. As shown in the following, magnetic structure is revealed *only* by MFISH.

SHG from χ_{xxxx}, χ_{zxxx}, and χ_{zzzx} is allowed in the magnetic point groups 1, $\underline{1}$, $\underline{2}$, m, $\underline{2}/m$, and eight trigonal or hexagonal groups [24]. The latter are incompatible with the tetragonal lattice, and groups $\underline{1}$ and $\underline{2}/m$ do not allow a ferromagnetic moment. Excluding monoclinic symmetry, only groups $\underline{2}$ and m remain. Group m points to a magnetic structure with twofold [110] axis and ferromagnetic moment parallel to this axis whereas group $\underline{2}$ points to a magnetic structure with mirror plane (100), (010), or (001) and in-plane ferromagnetic moment. Figure 4 and the ensuing discussion will show that the ferromagnetic moment can be oriented along the x or z axis by an external 50 mT field without further reduction of magnetic symmetry. This leaves $\underline{2}$ as magnetic symmetry with mirror plane xz and in-plane magnetic moment.

Using the lines at 1.410 and 1.875 eV as sublattice selective probes for the 4b and 8d sites, dependence of the MFISH signal on temperature and magnetic field is shown in Fig. 4. For the 4b site the MFISH intensity at $10 < T < 21$ K is saturated at 50 mT which indicates saturation of the weak ferromagnetic moment accompanying antiferromagnetic order. Consequently the intensity of the line at 1.410 eV reproduces the temperature dependence of the magnetic order parameter. For the 8d site, however, the line at 1.875 eV indicates abnormal behavior because both ferromagnetic *and* paramagnetic behavior are observed depending on choice of, respectively, x or z as detected polarization of the MFISH signal. Obviously the Cu^{2+} ions at 4b sites impose their magnetic order onto the Cu^{2+} ions at 8d sites where it coexists with a disordered paramagnetic component. Contrary to contemporary belief [14,16,19,20] the 4b and 8d sublattices are therefore strongly coupled even above 10 K.

At $\mu_0 H \lesssim 1$ T only A- and C-type MFISH are observed. However, at $\mu_0 H > 1$ T Fig. 4 shows B-type

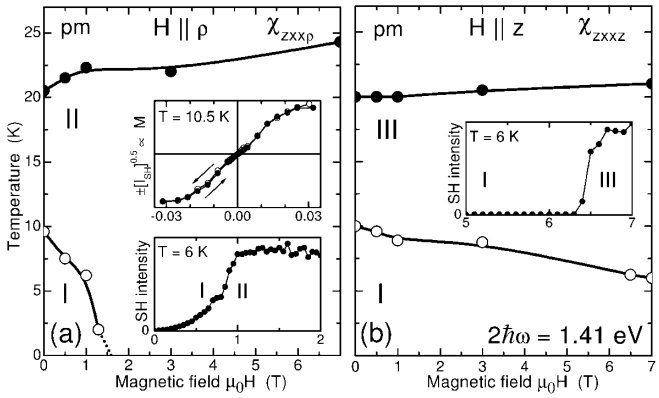

FIG. 5. Phase diagrams of CuB_2O_4 in the magnetic field/temperature plane for (a) in-plane ($H \parallel \rho$ with $\rho = x + y$) and (b) uniaxial ($H \parallel z$) magnetic fields. Insets: SH intensity I_{SH} or magnetization $M \propto \pm I_{SH}^{0.5}$ in dependence of the magnetic field for selected points in the phase diagram.

MFISH from field induced phase transitions. Two plots with $H \perp z$ and $H \parallel z$ complete the magnetic phase diagram of CuB_2O_4 in Fig. 5 because dependence of phase boundaries on the direction of H in the xy plane was found to be negligible. In the magnetic field the incommensurate purely antiferromagnetic phase I is engulfed by the weakly ferromagnetic commensurate phase with a different direction of magnetization in phases II and III. At 0 K quenching occurs at the extrapolated field $\mu_0 H_x = 1.6$ T (I $\rightarrow$ II) or $\mu_0 H_z = 30$ T (I $\rightarrow$ III), the transitions being, respectively, of second or first order with gradual or abrupt reorientation of spins (see insets). Recent neutron diffraction data [28] revealed a magnetic phase transition for $\mu_0 H = 1.3$ T with $H \parallel [110]$ at 4.2 K in excellent agreement with our data.

In conclusion, observation of the giant MFISH generation opens new degrees of freedom for probing the magnetic and electronic properties of matter. Using the two-sublattice compound CuB_2O_4 as a model system we detect unusually sharp and intense spectral lines both in linear absorption and MFISH spectra which provide site selective access to the electronic and magnetic structure of CuB_2O_4 by the appropriate choice of photon energy. However, only the MFISH signal is sensitive to magnetic structure and reveals commensurate and incommensurate antiferromagnetic ordering with or without a weak ferromagnetic component for the 4*b* site. Strong intersublattice coupling imposes this order onto magnetic moments at the 8*d* site where it coexists with a discoupled paramagnetic component of the Cu^{2+} moment. Spontaneous and magnetic-field induced phase transitions are observed and magnetic phase diagrams are derived. A highly anisotropic behavior with generally low stability of the incommensurate phase is observed.

The authors thank the Russian Foundation for Basic Research and the Deutsche Forschungsgemeinschaft for financial support. Technical assistance by H.-J. Weber and O. Schöps in absorption measurements is appreciated. M. F. thanks Th. Elsässer and M. Bayer for continuous support.

*Electronic address: fiebig@mbi-berlin.de

[1] Y. R. Shen, *The Principles of Nonlinear Optics* (Wiley, New York, 1984).
[2] R. W. Boyd, *Nonlinear Optics* (Academic, San Diego, 1992).
[3] *Nonlinear Optics in Metals*, edited by K. H. Bennemann (Clarendon, Oxford, 1998).
[4] *Nonlinear Spectroscopy of Solids: Advances and Applications*, edited by B. Di Bartolo (Plenum, New York, 1994).
[5] Y. Uesu, S. Kurimura, and Y. Yamamoto, Appl. Phys. Lett. **66**, 2165 (1995).
[6] M. Fiebig, D. Fröhlich, B. B. Krichevtsov, and R. V. Pisarev, Phys. Rev. Lett. **73**, 2127 (1994).
[7] C. H. Lee, R. K. Chang, and N. Bloembergen, Phys. Rev. Lett. **18**, 167 (1967).
[8] M. M. Fejer, G. A. Magel, D. H. Jundt, and R. L. Byer, IEEE J. Quantum Electron. **28**, 2631 (1992).
[9] V. Venkataramanan, K. Noguchi, M. Aono, and T. Suzuki, Appl. Phys. B **74**, 683 (2002).
[10] M. Fiebig, D. Fröhlich, and H. J. Thiele, Phys. Rev. B **54**, 12 681 (1996).
[11] M. Fiebig, Th. Lottermoser, and R. V. Pisarev, J. Appl. Phys. **93**, 8194 (2003).
[12] A. Kirilyuk, J. Phys. D **35**, R189 (2002).
[13] A. N. Bogdanov, U. K. Rößler, M. Wolf, and K. H. Müller, Phys. Rev. B **66**, 214410 (2002).
[14] B. Roessli *et al.*, Phys. Rev. Lett. **86**, 1885 (2001).
[15] G. A. Petrakovskii, A. D. Balaev, and A. M. Vorotinov, Phys. Solid State **42**, 321 (1999).
[16] M. Boehm, S. Martynov, B. Roessli, G. Petrakovskii, and J. Kulda, J. Magn. Magn. Mater. **250**, 313 (2002).
[17] M. Martinez-Ripoli, S. Martinez-Carrera, and S. Garcia-Blanco, Acta Crystallogr. Sect. B **27**, 677 (1971).
[18] G. F. Koster, J. O. Dimmock, R. G. Wheeler, and H. Statz, *Properties of the 32 Point Groups* (MIT Press, Cambridge, 1963).
[19] G. A. Petrakovskii, M. A. Popov, B. Roessli, and B. Ouladdiaf, J. Exp. Theor. Phys. **93**, 809 (2001).
[20] H. Nakamura, Y. Fujii, H. Kikuchi, and M. Chiba (to be published).
[21] A. I. Pankrats *et al.*, JETP Lett. **78**, 569 (2003).
[22] G. A. Petrakovskii, K. A. Sablina, D. A. Velikanov, A. M. Vorotinov, N. V. Volkov, and A. F. Bovina, Crystallogr. Rep. **45**, 853 (2000).
[23] M. Fiebig, D. Fröhlich, Th. Lottermoser, V. V. Pavlov, R. V. Pisarev, and H. J. Weber, Phys. Rev. Lett. **87**, 137202 (2001).
[24] R. R. Birss, *Symmetry and Magnetism* (North-Holland, Amsterdam, 1966).
[25] Y. Tokura *et al.*, Phys. Rev. B **41**, 11 657 (1990).
[26] M. Bassi *et al.*, Phys. Rev. B **54**, 11 030 (1996).
[27] Y. Okimoto, Y. Tomioka, Y. Onose, Y. Otsuka, and Y. Tokura, Phys. Rev. B **57**, 9377 (1998).
[28] J. Shefer, M. Boehm, B. Roessli, G. A. Petrakovskii, B. Ouladdiaf, and U. Staub, Appl. Phys. A **74**, 1740 (2002).